

Observing community resilience from space: Using nighttime lights to model economic disturbance and recovery pattern in natural disaster

Yi Qiang^{a,*}, Qingxu Huang^b, Jinwen Xu^a

^a Department of Geography and Environment, University of Hawaii – Manoa, USA

^b Center for Human-Environment System Sustainability (CHESS), State Key Laboratory of Earth Surface Processes and Resource Ecology (ESPRE), Beijing Normal University, China

ARTICLE INFO

Keywords:

Natural disaster
Resilience
Economic recovery
Nighttime lights
Empirical assessment
DMSP/OLS

ABSTRACT

A major challenge for measuring community resilience is the lack of empirical observations in disasters. As an effective tool to observe human activities on the earth surface, night-time light (NTL) remote sensing images can fill the gap of empirical data for measuring community resilience in natural disasters. This study introduces a quantitative framework to model recovery patterns of economic activity in a natural disaster using the Defense Meteorological Satellite Program-Operational Linescan System (DMSP-OLS) images. The utility of the framework is demonstrated in a retrospective study of Hurricane Katrina, which uncovered the great economic impact of Katrina and spatial variation of the disturbance and recovery pattern of economic activity. Environmental and socio-economic factors that potentially influence economic recovery were explored in statistical analyses. Instead of a static and holistic index, the framework measures resilience as a dynamic process. The analysis results provide actionable information for prompting resilience in diverse communities and in different phases of a disaster. In addition to Hurricane Katrina, the resilience modeling framework is applicable for other disaster types. The introduced approaches and findings increase our understanding about the complexity of community resilience and provide support for developing resilient and sustainable communities.

1. Introduction

Due to climate change and rapid population growth, human society is faced with increasing threats from natural disasters that can cause significant socio-economic consequences. Coastal communities around the world are particularly vulnerable to natural disasters including both large-scale rapid-moving disturbances such as hurricane and storm surges (Tebaldi, Strauss, & Zervas, 2012), and the slow-moving processes such as coastal erosion, sea level rise (Nicholls, Hoozemans, & Marchand, 1999) and reduction of ecosystem services (Spalding et al., 2014). According to the data from U.S. Census Bureau (2011), 39 % of the total population in the United States are living in counties directly on the shorelines and the population density in coastal counties is more than four times the average density of the whole United States. Since 2005 when Hurricane Katrina and Rita caused catastrophic damage in Central Gulf Coast, much attention has been paid to the resilience and long-term sustainability of coastal communities. Empirical observations suggest that, under the same strength of disasters, different communities endured different levels of disturbance and presented different recovery patterns in socio-economic (Finch, Emrich, & Cutter, 2010;

Fussell, Sastry, & VanLandingham, 2010), health (Burton, 2006; Sastry & VanLandingham, 2009), and psychological conditions (Adeola, 2009). These observed disparities can be attributed to various resilience of the communities.

Resilience describes the ability of an individual or a system to adapt to and recover from external shocks or stresses (Adger, 2000). Although substantial knowledge has been gained on ecological resilience (Perz, Muñoz-Carpena, Kiker, & Holt, 2013) and engineering resilience (Yodo & Wang, 2016), there is yet a consensus on how to measure resilience of human communities due to their complexity. In general, quantitative assessment of community resilience is challenged by two issues. First, the definition of community resilience varies in different domains, which will be discussed in Section 2.1. Moreover, resilience is often used interchangeably with other relevant concepts such as vulnerability and adaptive capacity. The various definitions and conceptual frameworks of community resilience influence how researchers measure resilience (Cutter et al., 2008; Lam, Reams, Li, Li, & Mata, 2016; Sherrieb, Norris, & Galea, 2010). The definition disagreement hampers the development of standard metrics to measure resilience. Second, there is lack of empirical data and approaches to quantify community

* Corresponding author.

E-mail addresses: yiqiang@hawaii.edu (Y. Qiang), qxhuang@bnu.edu.cn (Q. Huang), jinwenxu@hawaii.edu (J. Xu).

resilience. Most of the existing assessments are based on an index approach, which integrates a set of presumed indicators into a composite score to measure resilience (Cutter, Burton, & Emrich, 2010; Hung, Yang, Chien, & Liu, 2016; Sempier, Swann, Emmer, Sempier, & Schneider, 2010; Sherrieb et al., 2010). The model specification, indicator selection and weighting are based on prior knowledge or expert opinions. Although these indices provide general guidance for predicting community resilience, their accuracies have not been validated against empirical observations in disasters (Bakkensen, Fox-Lent, Read, & Linkov, 2017; Beccari, 2016).

Empirical data about human activities and states are difficult to obtain in a disaster condition when many social systems fail to function. Traditional data sources for resilience assessment (e.g. surveys and census data) have limitations in various aspects, which will be elaborated in the next section. Recently, remote sensing imageries become popular instruments to monitor human dynamics on the earth surface such as urban growth (Shahtahmassebi et al., 2016), land cover change (Joshi et al., 2016), and socio-economic conditions (Kuffer, Pfeffer, & Sliuzas, 2016). Among the various remote sensing products, night-time light (NTL) remote sensing has unique ability to capture fluctuations of human activities, which can provide empirical data for resilience assessment. This study introduces a quantitative framework to assess community resilience using the DMSP-OLS NTL annual composite images as the data source. Specifically, stable lights in the time series of DMSP-OLS annual images are used as a proxy to model recovery patterns of economic activity after Hurricane Katrina in 2005. Spatial and statistical analyses are conducted to explore the geographical disparities of the recovery patterns and their relationships with the selected resilience indicators. Specific questions answered in the case study are: 1) which communities appeared to be more or less resilient in the disaster; 2) how the observed resilience levels are associated with the environmental and socio-economic conditions? The introduced framework aims to fill the critical gap of empirical data and assessment methods for community resilience. The analysis results from the case study increase our understanding about community resilience and provide actionable information to predict and prompt community resilience.

The rest of the article is organized as follows. Section 2 briefly reviews the related work about the definitions, conceptual frameworks and assessment methods of community resilience. Section 3 introduces the data sources, assessment framework of community resilience based on NTL data and statistical analyses. Section 4 presents the analysis results in the case study of Hurricane Katrina, followed by the discussions in Section 5 and conclusions in Section 6.

2. Related work

2.1. Definition and conceptual framework

The concept of resilience was first introduced by Holling (1973), who views resilience as the ability of an ecological system to absorb change in the face of extreme perturbation and yet continue to persist. Later, Timmerman (1981) applied the concept of resilience to social systems and defined resilience as the measure of a system's capacity to absorb and recover from disastrous events. The resilience of a social system is also known as community resilience. Extending Timmerman's definition, Cutter et al. (2008) further elaborated that community resilience includes both the inherent conditions of a system to absorb impacts and cope with an event and post-event, adaptive processes that facilitate the ability of the social system to re-organize, change, and learn in response to a threat. Norris, Stevens, Pfefferbaum, Wyche, and Pfefferbaum (2008) considered resilience as a process linking communities' capacities in response to the disturbance. In the field of engineering and infrastructure systems, resilience describes the ability of resisting and absorbing disturbances and the ability of adapting to disruptions, and returning to normal functionalities (Faturechi & Miller-

Hooks, 2015). Extensive reviews about the definitions of resilience and the related terms can be found in (Cutter et al., 2008; Lam et al., 2016; Liao, 2012; Peacock, 2010). Despite the various definitions in the literature, community resilience is often associated with two abilities: 1) the ability to absorb/resist/withstand disturbance, and 2) the ability to respond/recover/restore the acceptable level of functioning and structure.

In addition to the qualitative descriptions, a number of theoretical frameworks have been developed to quantify community resilience. For instance, Cutter et al. (2010), Cutter, Ash, & Emrich (2014) define that resilience consists of six components including social, economic, infrastructural, institutional, community, and environmental, which is used as a guidance to select indicators for resilience indices. Lam et al. (2016) measure resilience from the relationships among exposure, damage and recovery. Additionally, resilience can be conceptualized as a dynamic process such as the recovery trajectory (also known as recovery curve), which describes the continuous change of a functional capacity of a system affected by a disturbance (e.g. natural disaster). The functional capacity could be the social and economic capacity of a human community (White, Edwards, Farrar, & Plodinec, 2015), biomass or population of an ecological community (Qiang & Xu, 2019; Vercelloni, Kayal, Chancerelle, & Planes, 2019), or the functionality or serviceability of an infrastructure system (Koliou et al., 2018). The Curve A, B and C in Fig. 1 illustrates common scenarios of resilience from high to low, where the functional capacity suddenly declines after a disturbance, gradually recovers afterwards, and finally restores to the pre-disaster condition (e.g. Trajectory B) or a new equilibrium (Trajectory A and C). Given the same strength of disaster, the variation of the recovery trajectory is indicative of community resilience. The maximum deviation from the pre-disaster condition (i.e. maximum disturbance) reflects the ability of a system to absorb/resist/withstand disturbance from the disaster. The recovery speed or time indicates the ability to respond/recover/restore the functional capacity.

2.2. Resilience assessment – index approaches

Previous work of resilience assessment is mostly based on an index approach, which aggregates a number of socio-economic and environmental indicators into an overall resilience index. The Baseline Resilience Index for Communities (BRIC) developed by Cutter et al. (2010) is one of the first and most cited resilience index. Analogous to the previous work of the Social Vulnerability Index (SoVI) (Cutter, Boruff, & Shirley, 2003), BRIC is aggregated from 36 indicators of the baseline characteristics of community resilience. The indicators are rescaled into [0,1] and then aggregated in five categories including social, economic, institutional, infrastructure, and community. The overall BRIC index is the summation of the aggregated indices in the

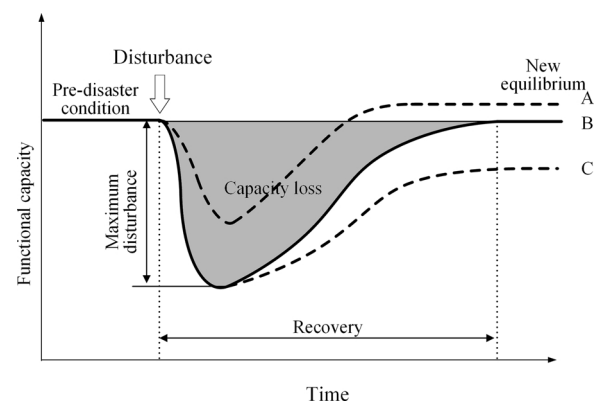


Fig. 1. Recovery trajectory of a system due to an external disturbance. Curve A, B and C represent three possible scenarios of resilience from high to low. (Modified from White et al., 2015)

five categories. Analogously, the Community Disaster Resilience Index (CDRI) by (Peacock, 2010) categorizes resilience indicators into a 4×4 matrix with capital domains (i.e. the social, economic, physical, and human capital) and disaster phases (i.e. the mitigation, preparedness, response and recovery phase). The selected indicators are aggregated in 16 categories in the matrix, which are then aggregated into the CDRI index. Other work on resilience indices include (Foster, 2012; Hung et al., 2016; Sherrieb et al., 2010). Although these indices provide general predictions of resilience by integrating prior knowledge and expert opinions, they do not inform specific disaster outcomes. For instance, it is unclear whether a high resilience index implies low property loss, low casualty and injury, or fast economic recovery. The unspecified outcomes diminish the value of the indices for specific decision-making. Moreover, most of the resilience indices have not been calibrated or validated against empirical observations. Bakkensen et al. (2017) validated the BRIC and CDRI with observed losses, fatalities, and disaster declarations, and found low or even contradictory correlations between the indices and disaster outcomes.

2.3. Resilience assessment – empirical approaches

In addition to the index approach, efforts have been made to assess community resilience using empirical observations in disasters. For instance, Lam, Pace, Campanella, LeSage, and Arenas (2009) and LeSage, Pace, Lam, Campanella, and Liu (2011) conducted a series of telephone and street surveys to continuously monitor business reopening in New Orleans after Hurricane Katrina. The time series of open businesses resemble the recovery trajectory illustrated in Fig. 1, which declines sharply after Katrina and gradually recovers afterwards. The various recovery patterns in different communities were associated with environmental and socio-economic variables to explain why some communities restored businesses more quickly than others. However, the surveys were costly, labor-intensive and time consuming, which is not widely applicable. Later, (Lam, Qiang, Arenas, Brito, & Liu, 2015; Lam, Reams, Li, Li, & Mata, 2016) developed the Resilience Inference Model (RIM) which uses the number of disasters, damage and population growth as proxies to measure community resilience. Based on aggregated data in a 10-year period, the RIM model considers that a resilient community can resist damage and maintain high population growth while endured a high number of disasters. Recently, with the advent of the Big Data era, data crowdsourcing and social media platforms provide new opportunities to observe individuals' activities and narratives at finer spatial and temporal resolutions. For instance, Zou, Lam, Cai, & Qiang (2018) used the frequency and sentiment of geo-tagged Twitter messages (tweets) to monitor dynamic conditions of communities in Hurricane Sandy. The recovery trajectories of communities can be reflected from time series of ratios and average sentiment of tweets during the disaster. Timeliness, low cost and scalability are the main advantages of social media data. However, the Big Data approaches are criticized for the biased user profile (Zou, Lam, Shams et al., 2018) and low data quality (much noise and misinformation) (Li et al., 2016).

2.4. Remote sensing for disaster management

Remotely sensed imageries have been widely applied in disaster risk mapping (Bates, 2004; Hong, Adler, & Huffman, 2007) and damage assessment (Cooner, Shao, & Campbell, 2016; Dong & Shan, 2013; Vetrivel, Gerke, Kerle, Nex, & Vosselman, 2018). However, most remote sensing products are not very useful for resilience assessment due to their insensitivity to decline of human activity. For instance, it is difficult to detect a 'ghost town' or a damaged city from Landsat images. As an alternative, nighttime light (NTL) remote sensing images have been proved an effective means to observe the dynamics (both increase and decline) of population (Zhuo et al., 2009), urbanization (Xie & Weng, 2017) and economic activities (Li, Ge, & Chen, 2013). A

comprehensive review of applications of NTL data can be found in (Huang, Yang, Gao, Yang, & Zhao, 2014). For disaster management, the NTL data have been applied to identify damage (Gillespie, Frankenberg, Chum, & Thomas, 2014; Kohiyama et al., 2004), power outage (Hultquist, Simpson, Cervone, & Huang, 2015; Zhao et al., 2018), and analyze the change of human activities (Li, Zhan, Tao, & Li, 2018) and urbanization (Huang, Wang, & Lu, 2019) affected by disasters. Despite these applications, the utility of NTL data in modeling community resilience has not been fully exploited in a theoretical framework. Extending the conceptual framework of recovery trajectory, this study introduces a quantitative approach to model resilience using DMSP/OLS NTL images as the data source.

3. Method

3.1. Inter-calibration of NTL images

The Stable Lights images collected by the Defense Meteorological Satellite Program Operational Line Scanner (DMSP/OLS) were used for this study. The images are cloud-free composites created using all the available archived DMSP-OLS smooth resolution data from the year 1992 to 2013. The DMSP/OLS images include 34 annual composites at a 30 arc second resolution collected by six different satellites (F10, F12, F14, F15, F16, and F18). Due to the absence of inter-satellite calibration and onboard calibration, the digital numbers (DN) in the DMSP-OLS images cannot be converted to exact radiance. To analyze continuous recovery trajectories over time, the DMSP-OLS images need to be calibrated to make the images in different years and satellites comparable. A widely applied inter-calibration procedure was proposed by (Elvidge et al., 2009), which uses a quadratic polynomial regression to adjust the DNs against a reference image (see Eq. (1)).

$$DN_{\text{calibrated}} = a_1 + a_2 \cdot DN + a_3 \cdot DN^2 \quad (1)$$

The inter-calibration process follows the same procedure as introduced in (Elvidge et al., 2009). By reviewing the data, it was found that the image F121999 has the highest average DN in the United States. Due to the saturation of the DMSP/OLS in bright areas (e.g. city centers), the F121999 was used as the reference image and all other images were calibrated to match the DNs in F121999. Los Angeles was chosen as the reference site, as it has been a mature metropolis where the light change is negligible (Hsu, Baugh, Ghosh, Zhizhin, & Elvidge, 2015). Due to the uneven distribution of DNs in the images, a random sampling will lead to overfit near the two extremes of DNs (i.e. 1 and 63) where pixels are concentrated. To ensure the regression equations evenly fit the entire value range, a stratified sample of lit pixels (200 pixels in each DN value) were extracted in the reference site for the calibration. The 2nd order regression equation was calibrated for each image with the reference to F121999. The coefficients of the regression equations are in Table 1. After the calibration, images in the same year were averaged into one image, leading to a time series of annual images from 1992 to 2013.

3.2. Estimation of gross domestic product

The inter-calibrated DMSP-OLS images were clipped in the affected area in Hurricane Katrina, which include 179 counties declared as disaster areas by the Federal Emergency Management Agency (FEMA). Hurricane Katrina made the first landfall in Florida on August 25th, 2005 and the second in Louisiana on August 29th, 2005. The disaster areas include the entire Louisiana (64 parishes) and Mississippi (82 counties), 22 counties in Alabama, and 11 counties in Florida (Fig. 2). Zonal operation was applied to aggregate the DNs in the counties. After logarithm transformation, the sum of DNs and number of lit pixels can well predict ($R^2 = 0.92$) the gross domestic product (GDP) in the 179 counties in a linear model (Eq. (2)). The goodness of fit (i.e. R^2) is highest for GDP compared to other economic indicators (e.g. personal

Table 1
Coefficients of the quadratic polynomial regression for inter-calibration.

Satellite	Year	a_1	a_2	a_3	R^2
F10	1992	0.99490	1.19694	-0.00419	0.84241
F10	1993	-0.53668	1.51570	-0.00845	0.90954
F10	1994	1.09383	1.46457	-0.00852	0.87570
F12	1994	0.68785	1.22501	-0.00428	0.88668
F12	1995	1.29538	1.19446	-0.00428	0.88056
F12	1996	0.52894	1.33022	-0.00633	0.87521
F12	1997	1.47600	1.18090	-0.00472	0.83470
F12	1998	0.92953	1.08940	-0.00259	0.92079
F12	1999	1	1	1	1
F14	1997	2.04904	1.55982	-0.01079	0.85754
F14	1998	0.94451	1.55107	-0.00977	0.95204
F14	1999	0.80845	1.52425	-0.00911	0.95928
F14	2000	2.42372	1.29577	-0.00605	0.90692
F14	2001	2.51390	1.43262	-0.00829	0.91364
F14	2002	3.59977	1.34024	-0.00760	0.87948
F14	2003	3.05182	1.37950	-0.00788	0.90928
F15	2000	0.55891	1.15751	-0.00315	0.94024
F15	2001	0.57387	1.23965	-0.00433	0.93629
F15	2002	1.30027	1.19630	-0.00416	0.93331
F15	2003	1.86389	1.64457	-0.01154	0.92080
F15	2004	2.74263	1.56383	-0.01043	0.90945
F15	2005	2.51648	1.55181	-0.01034	0.88839
F15	2006	2.94339	1.38264	-0.00811	0.86845
F15	2007	3.99771	1.41246	-0.00897	0.82033
F16	2004	2.32112	1.37760	-0.00795	0.87267
F16	2005	2.90092	1.56247	-0.01079	0.87283
F16	2006	2.64689	1.25093	-0.00583	0.85792
F16	2007	2.83160	1.15147	-0.00477	0.84669
F16	2008	2.94479	1.17826	-0.00534	0.81480
F16	2009	2.36856	1.24705	-0.00609	0.84942
F18	2010	2.35041	0.94747	-0.00196	0.80366
F18	2011	1.63669	1.20682	-0.00557	0.85396
F18	2012	2.56954	1.07559	-0.00385	0.82972
F18	2013	2.25727	1.07572	-0.00365	0.85132

income, number of employees and business establishments). As county-level GDP data in the U.S. is only available in 2012–2015 (Bureau of Economic Analysis, U.S. Department of Commerce, 2018), the GDP data and DMSP-OLS images in 2012 and 2013 (the overlapping years of the two data sources) were used to derive the regression equation. All the GDP data are adjusted to the value of current U.S. dollar. Finally, the GDP of the counties from 1992 to 2013 was estimated using Eq. (3).

$$\log(GDP_{2003,2004}) = 3.375 \cdot \log(DN_{sum}) - 2.548 \cdot \log(lit_{DN}) - 1.761 \quad (2)$$

$$GDP_{1992-2013} = e^{(3.375 \cdot \log(DN_{sum}) - 2.548 \cdot \log(lit_{DN}) - 1.761)} \quad (3)$$

3.3. Measurement framework

The estimated GDP was analyzed in the framework in Fig. 3 to assess the resilience of the counties. The GDP of each county is rescaled into [0, 1] to be comparable. Two regression lines were derived for the normalized GDP from 1992 to 2004 and from 2005 to 2013 to represent the pre- and post-Katrina economic trajectory respectively. Although various models are available for GDP projection, the linear model is still considered a valid benchmark to project GDP growth in the U.S. (Ferrara, Marcellino, & Mogliani, 2015; Marcellino, 2008), especially in the recent decades when the volatility of US GDP growth tend to decline (Burren & Neusser, 2010). Despite the slight decline (-1.8 %) in 2009 due to the financial crisis, the annual GDP in the U.S. from 1990 to 2018 generally follows a linear trend (World Bank, 2019). The extension of the pre-Katrina trajectory (thin dashed line in Fig. 3) represents the business-as-usual condition as if the pre-Katrina economic growth persists.

Three metrics were calculated for each county. First, the difference between the projected GDP in the business-as-usual trajectory ($f_{pre}(2005)$) and the actual 2005 GDP in the post-Katrina trajectory

($f_{post}(2005)$) was calculated to represent instant economic disturbance caused by Katrina (Eq. (4)). This metric (denoted as D for simplicity) measures the ability of a system to absorb/resist/withstand disturbance in a disaster. Second, the difference between the slope of the post-disaster trajectory (r_2) and the slope of business-as-usual trajectory (r_1) was calculated to indicate the recovering rate (R_r) of GDP after Katrina (Eq. (5)). A high (positive) R_r would implies a strong ability to respond/recover/restore the GDP growth to catch up with the business-as-usual trajectory. Third, the accumulated difference between the post-disaster GDP and the business-as-usual GDP from 2005 to 2013 was calculated using Eq. (6). This metrics measures the accumulated economic loss (L) due to the deviation of GDP growth from the business-as-usual trajectory, which is illustrated as the grey area in Fig. 3. L represents the combined effect of D and R_r . A high L can be interpreted as low resilience, which typically consists of a high instant disturbance (D) and slow recovery (R_r). A low L means the opposite. L differentiates the intermediate situations such as high D and high R_r , or low D and low R_r . L is calculated from 2005 to 2013 after Katrina when the DMSP-OLS images are available.

$$D = f_{pre}(2005) - f_{post}(2005) \quad (4)$$

$$R_r = r_2 - r_1 \quad (5)$$

$$L = \int_{2005}^{2013} (f_{pre}(t) - f_{post}(t)) \quad (6)$$

3.4. Regression analysis

Regression analyses were applied to examine the associations of the three resilience metrics (D , R_r and L) with environmental and socio-economic variables. The selected variables fall into four categories, including impact intensity, environmental, socio-economic, and industrial structure. Max wind gust speed and accumulated rainfall represent the destructive power of a hurricane (NOAA, 2006). Elevation, proximity to coast and ratio of urban in flood zones indicate the exposure to Hurricane-induced storm surge and flooding (Dasgupta, Laplante, Murray, & Wheeler, 2011; Jonkman, Maaskant, Boyd, & Levitan, 2009). The socio-economic category includes 10 commonly used indicators in community resilience measurements (Cai, Lam, Zou, & Qiang, 2018; Cutter et al., 2014). Ratios of establishments in different scales and industrial sectors represent the industry structure, which potentially influences economic recovery (Martin & Sunley, 2015). Most of the variables were acquired from datasets released before 2005 to represent pre-disaster conditions. Variables that are not reported in counties were preprocessed and averaged into counties (Table 2). Instead of composing a comprehensive index for resilience, the objective of the analysis is examining the relationships between the GDP recovery trajectories and the hypothetical resilience indicators.

Two types of regression analysis were carried out in this study. First, univariate regression was applied to examine the relationships between D , R_r and L and each individual variable. Second, multivariate regression was utilized to relate the three metrics with all the variables and variables in the four categories. R^2 of the multivariate regression indicates the proportion of variance explained by the different categories of variables. Adjusted R^2 were compared to evaluate the prediction power of the different categories for the recovery metrics. The regression analyses aim to explore the underlying factors that influence resilience and proportion of resilience variance that can be explained by the variables. All variables were re-scaled into z-scores for the regression analyses. Thus the b coefficient of the regression represents the direction and standard deviations of the relationship. The regression analyses were conducted in the linear model (lm) function in R.

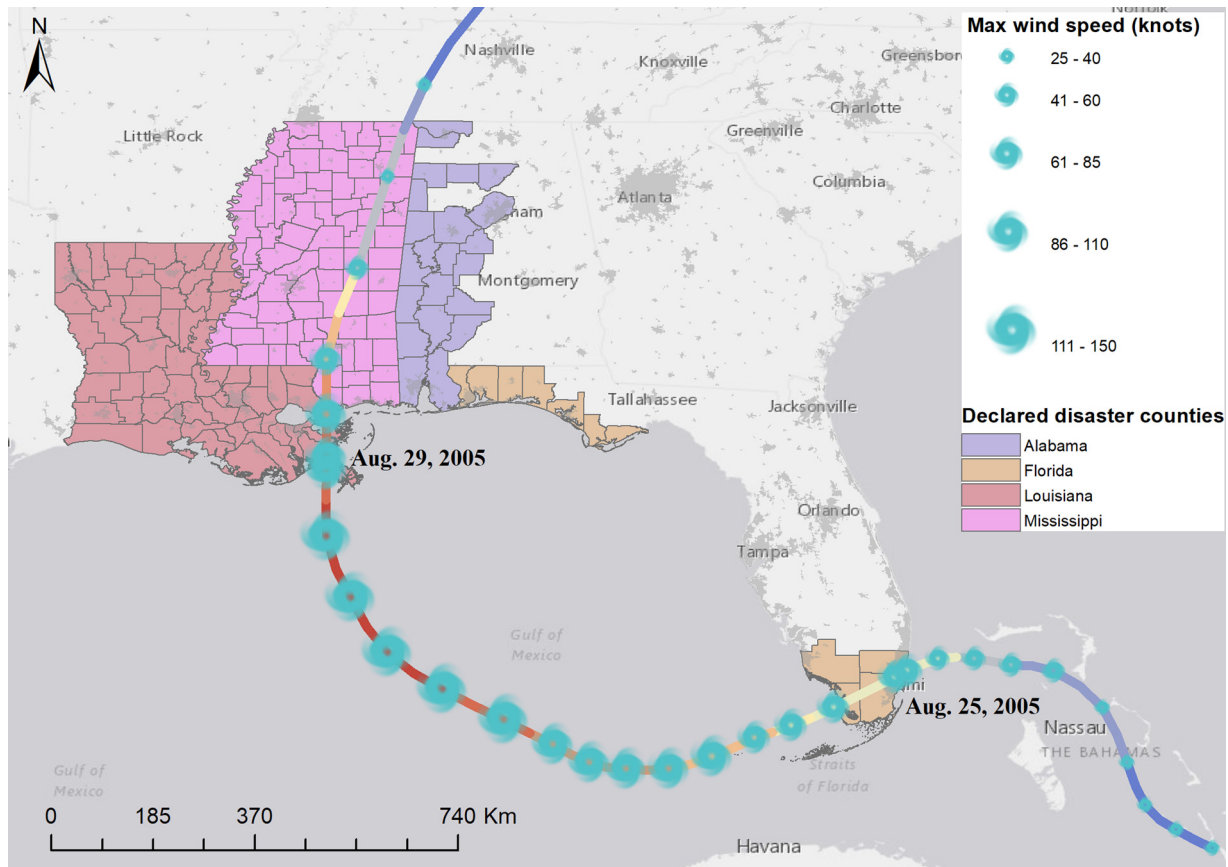


Fig. 2. The track of Hurricane Katrina and counties that are presidentially declared as disaster area.

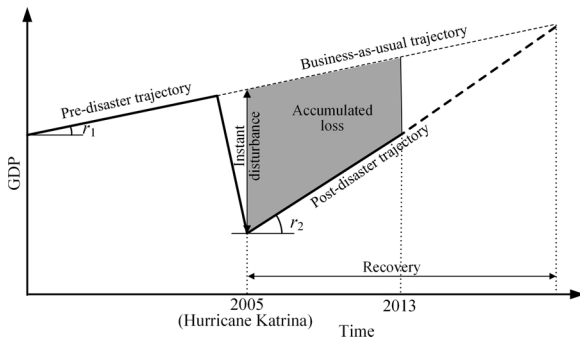


Fig. 3. Framework of GDP trajectory in Hurricane Katrina.

4. Result

4.1. Overall economic impact

Fig. 4 demonstrates the change of NTL brightness (DN value) from 2004 to 2005 near the landfall location of Katrina, where a decline of NTL brightness can be observed in New Orleans and the surrounding coastal cities. The annual GDP estimates from the NTL data (see Fig. 5) reveal that Hurricane Katrina has fundamentally altered the economic growth in the declared disaster area. In contrast to the steady growth in the Southeast Region (despite the slight drop in 2009 due to the financial crisis), the GDP in the disaster area declined sharply in 2005 and grew at a slower rate in the following years. The Southeast Region is delineated by Bureau of Economic Analysis, U.S. Department of Commerce (2015) for releasing economic statistics (see Fig. 2). According to our estimation, the GDP in 2005 in the entire disaster area declined 24.2 % compared with the business-as-usual condition if the

pre-Katrina growth trend persists. The accumulated loss of GDP from 2005 to 2013 (gray area in Fig. 5) is about 2.2 billion current dollar and the GDP is unlikely to restore to the business-as-usual trajectory in the following years. Note, this loss is estimated only from the declined GDP in the FEMA declared disaster area, which does not include other indirect losses in a broader area. Note, due to the instability of the DMSP-OLS images, the estimated GDP fluctuates from year to year. Although the estimation of GDP in a specific year may not be accurate, the general trend indicates the strong economic impact of the disaster.

4.2. Spatial variation of resilience

The GDP recovery trajectory varies in counties. As illustrated in Fig. 6, the estimated GDP in Orleans Parish (blue) and St. Bernard Parish (red) had a substantive decline in 2005 when Katrina stroke. Both parishes are in the metropolitan area of New Orleans near the landfall location of Katrina. The post-Katrina GDP in St. Bernard Parish shows a faster recovery rate than Orleans Parish after Katrina. In contrast, St. Tammany Parish (green) in the north shore of Lake Pontchartrain had little economic impact and maintained a steady GDP growth after Katrina, despite its proximity to the hurricane track.

As shown in Fig. 7 (a), Hurricane Katrina caused large instant disturbance (D) in counties near the two landfall locations in Florida and Louisiana. Note, the high D in southwest Louisiana (around Lake Charles Parish) is possibly due to Hurricane Rita, a Category 3 hurricane landed near the Louisiana-Texas border a month after Katrina. Fig. 7 (b) shows that Louisiana counties have a higher recovery rate (R_r) of GDP after Katrina, except Jefferson and Orleans Parish near the center of New Orleans which were struggling to recover after Katrina. High accumulated GDP loss (L) are distributed in coastal cities, including Gulfport (MS), Mobile (AL), Panama City and Miami (FL). The inland counties generally have lower accumulated loss.

Table 2
Description of variables used in the regression analyses.

Category	Variable	Description	Data source	Preprocessing
Impact intensity	Max gust	Recorded maximum gust speed from Aug. 23–30, 2005	Knobb et al. (2005)	Kriging interpolation, Zonal operation
	Rainfall	Total rainfall from Aug. 23–30, 2005	National Weather Service	Re-sampling, Zonal operation
Environmental	Mean elevation	Mean elevation	U.S. Geological Survey	Zonal operation
	Distance to Coast	Mean distance to coastline	NOAA	Euclidean distance, Zonal operation
	% of urban in flood zone	Percent of developed land in flood zone	FEMA flood map, National Land Cover Database	Method in (Qiang, 2019)
Socio-economic	% White	Percent of population in one race: White	U.S. decennial census (2000)	
	% Black	Percent of population in one race: Black or African American	U.S. decennial census (2000)	
	% Asian	Percent of population in one race: Asian	U.S. decennial census (2000)	
	% Hispanic & Latino	Percent of Hispanic or Latino population	U.S. decennial census (2000)	
	% children	Percent of population under 18 years old	U.S. decennial census (2000)	
	% elderly adult	Percent of population above 65 years old	U.S. decennial census (2000)	
	% owner occupied homes	Percent of owner occupied housing unit	U.S. decennial census (2000)	
	% bachelor degree	Percent of population (> 25 years old) with 4 or more years of college or bachelor's degree or higher	U.S. decennial census (2000)	
	% poverty	Percent of population whose income is below poverty level	U.S. decennial census (2000)	
Per cap. income	Per capita income	U.S. decennial census (2000)		
Industrial structure	% small businesses	Percent of establishments with < 20 employees	County business patterns (2004)	
	% large businesses	Percent of establishments with > 500 employees	County business patterns (2004)	
	% Agriculture	Percent of establishments in agriculture, forestry, fishing and hunting	County business patterns (2004)	
	% Mining	Percent of establishments in mining, quarrying, and oil and gas extraction	County business patterns (2004)	
	% Manufacture	Percent of establishments in manufacturing	County business patterns (2004)	

4.3. Regression analysis

Various relationships were found between the three metrics (D , R_r , L) and the selected variables (Table 3):

Instant disturbance (D) has the strongest relationship with the percent of Asian people (highest R^2) among the 20 selected variables. The positive coefficient b indicates that counties with a higher ratio of Asian people have endured greater GDP disturbance in Katrina. This result confirms the findings in Vu, VanLandingham, Do, and Bankston (2009) that 78 % of Vietnamese (the largest Asian group in Louisiana and Mississippi) left their home during the hurricane and gradually returns afterwards. D is also highly correlated with the physical impacts and environmental conditions. Specifically, counties with high gust speed, high accumulated rainfall, low elevation, high ratio of urban in flood zone, or close to the coastline tend to have a high D . This reflects the fact that New Orleans, which has low elevation and high ratio of urban flood exposure, was seriously damaged by flood inundation due to levee breach. Additionally, counties with a higher percentage of agricultural industry have a lower D .

High recovery rates (R_r) are associated with high percentages of energy industry (e.g. mining, quarrying, and oil and gas extraction), implying that the energy industry rebounded more quickly after the disturbance. Moreover, low elevation, proximity to coast, high ratios of children and elderly people tend to impede the GDP recovery.

Accumulated economic loss (L) is negatively correlated (highest R^2) with the ratio of owner-occupied housing units, indicating communities with more home-owner residents managed to prevent the overall economic loss. Communities with a higher ratio of Asian, Hispanic and Latino, children and elderly adults have suffered higher accumulated loss. High L is also found in counties with a high urban exposure to flood zone. Additionally, counties reliant on agricultural and mining industries tend to have a lower long-term loss.

R^2 of the multivariate regression indicates that the selected

variables can only explain 39.9 %, 29.3 % and 27.4 % variance of D , R_r , and L respectively (Table 4), which implies that other variables should be considered to model the recovery pattern. Due to the different numbers of variables in the four categories, adjusted R^2 was used to compare the variance explained by the different categories. In general, socio-economic variables can best predict (highest adjusted R^2) instant disturbance (D), followed by environmental condition and industrial structure. Industrial structure is the best indicator of recovery rate (R_r), followed by environmental and socio-economic variables. Socio-economic variables can best predict the accumulated economic loss (L). It is worth-noting that the disaster impacts explain the least variance in all the three metrics, which implies that the intrinsic community capacities (e.g. socio-economic conditions) are more decisive to economic recovery than the physical disaster impacts.

5. Discussion

Despite the extensive discussions in the literature, quantitative assessment of community resilience is still a challenge due to the lack of empirical data continuously collected in disasters. In the U.S, census data are released decennially and county-level GDP data is only available in limited years, not to mention the developing world. Other data collection methods such as field surveys and interviews are costly and time-consuming. As an alternative, NTL remote sensing is an efficient means to observe human activities (such as population, GDP, and energy consumption) from space. Most importantly, the NTL images have the unique ability to detect declines of human activities, which is not easy for other types of remote sensing imageries. The continuous scan of NTL images can capture the disturbance and recovery pattern of human activity during natural disasters at low cost and in a timely manner. The introduced framework can increase our understanding about community resilience and help to improve resilience prediction models in terms of variable selection and weighting.

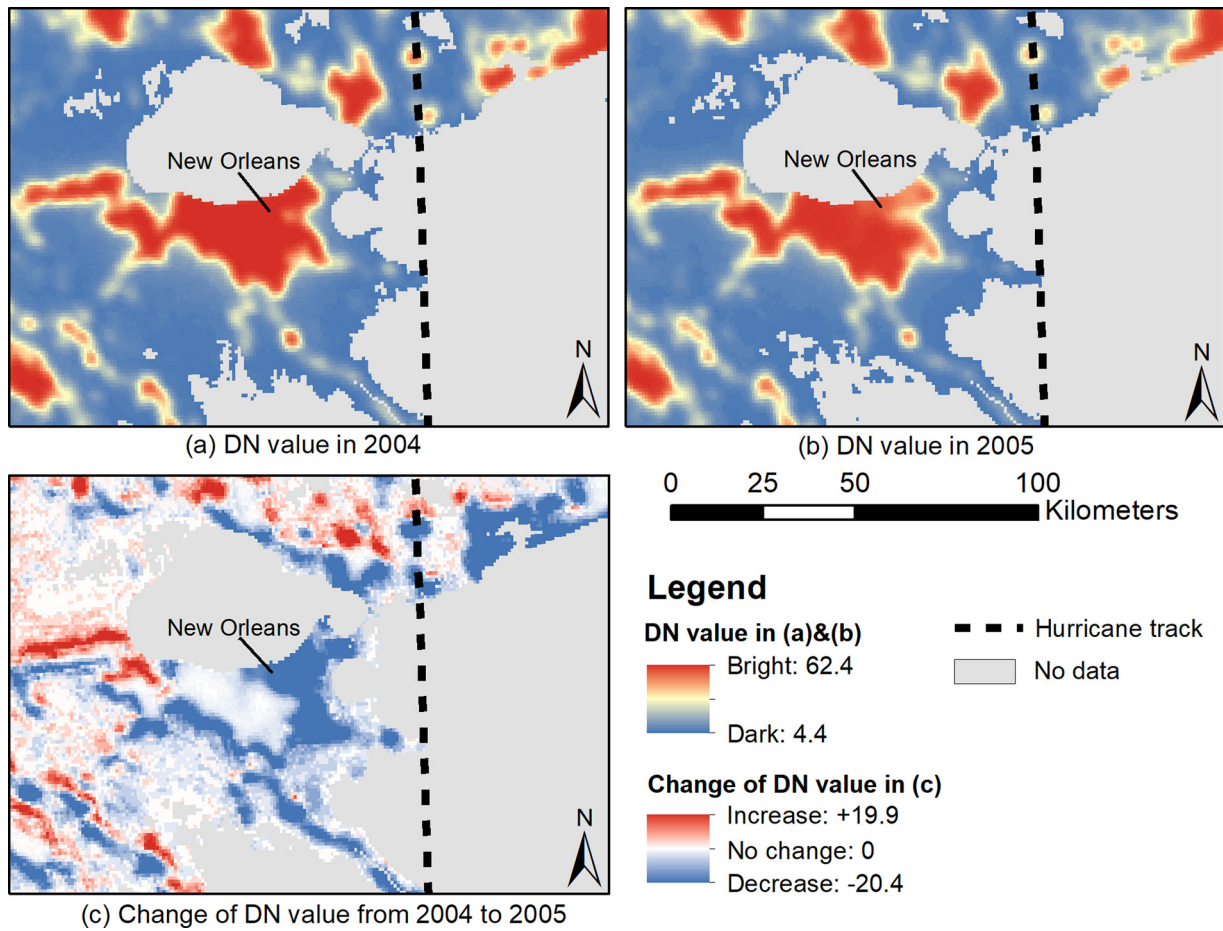


Fig. 4. Changes of NTL brightness (DN value) in the 2004 and 2005 DMSP-OLS annual composite images.

In addition to Hurricane Katrina, the introduced assessment framework based on NTL data is applicable to other natural disasters (e.g. tsunami and earthquake) that cause economic disturbance. The framework is particularly useful in situations where official socio-economic data are not available at the desired spatio-temporal resolution.

Not limited to the DMSP/OLS images, the introduced framework can use other data sources as input. For instance, the Visible Infrared Imaging Radiometer Suite (VIIRS) images, the new generation NTL remote sensing products since 2011, provide many new features (e.g. higher spatial and radiometric resolution) that are useful for measuring

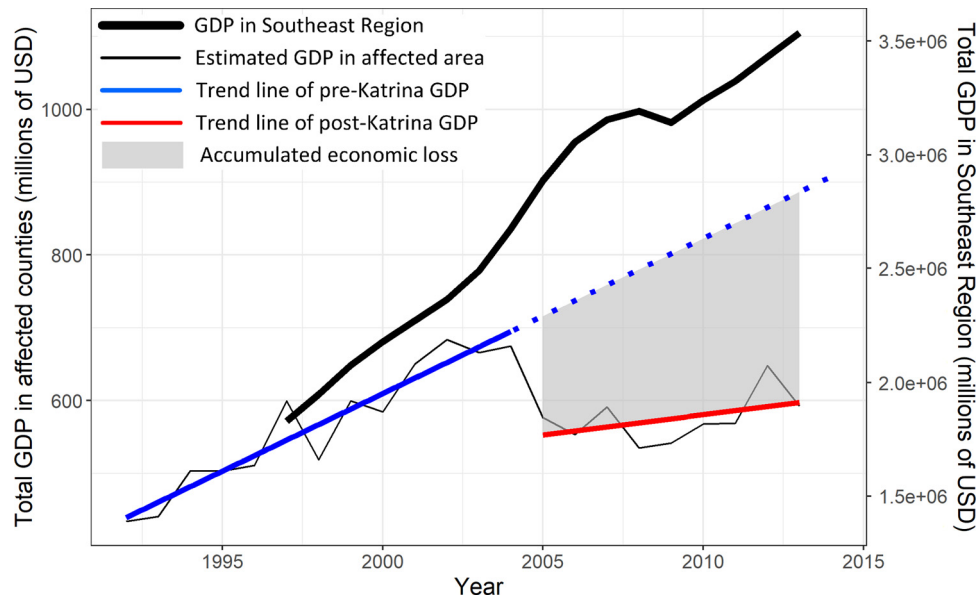


Fig. 5. Annual estimated GDP in current dollars in the affected area (refer to the left axis) and the Southeast Region (refer to the right axis) (Data source: Bureau of Economic Analysis).

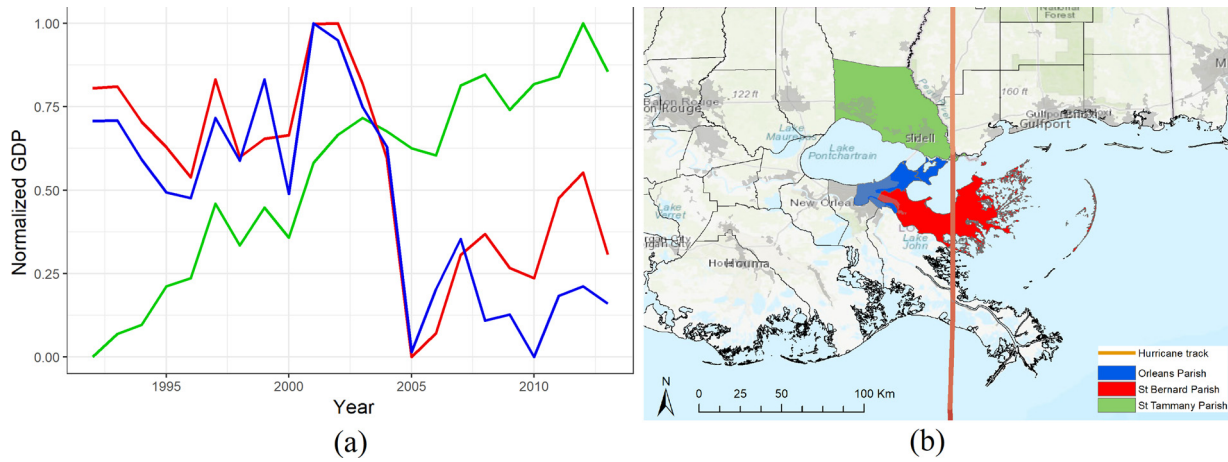


Fig. 6. Estimated GDP time series of Orleans Parish (blue), St. Bernard Parish (red) and St. Tammany Parish (green).

community resilience in disasters with a smaller impact area and shorter period.

As demonstrated in this study, the GDP time series estimated from the NTL data can capture the various recovery trajectories at the county level. The analysis results uncover the strong economic impact of Katrina in the affected region, where the GDP has given up its rapid growth and shifted to a different trajectory after 2005. This finding confirms the tremendous and long-lasting impact of Katrina on population migration (2010, Fussell, Curtis, & DeWaard, 2014), declined urban growth (Qiang & Lam, 2016) and economic activity (Baade, Baumann, & Matheson, 2007; Petterson, Stanley, Glazier, & Philipp, 2006). According to the recent estimates of the U.S. Census (2019), until 2017 the population and housing price in New Orleans has not yet recovered to the pre-Katrina level. The various GDP recovery patterns reveal geographical disparities of community resilience related to the local environmental and socio-economic conditions.

The recovery pattern of a social system is dependent on both intensity of disaster impacts and resilience of the system. The analysis results (see Table 4) suggest that the physical impact variables (including max gust speed and accumulated rainfall) can only explain limited variance ($R^2 = 0.065$) in the recovery pattern. Instead, the inherent conditions of communities (including environmental, socio-economic and industrial conditions) play a central role in shaping the recovery pattern. The univariate regression with individual variables provides empirical evidence about the underlying factors that influence the recovery. The results may also inform specific plans to prompt resilience at different phases of a disaster. For instance, the strong correlation between instant disturbance (D) and the environmental conditions (e.g. elevation, proximity to coast and % of urban area in flood zone) suggests that reducing exposure is the most effective way to reduce the direct impact caused by disasters. In the recovery phase,

communities with some demographic and socio-economic characteristics may have difficulties to bounce back, pinpointing areas where special assistance or policy levers should be applied. Compared with the traditional resilience indices without specific outputs, these analysis results can provide more actionable information to support decision-making at different phases of a disaster.

Despite the merits demonstrated in this study, the introduced approach can be improved in the following aspects. First, despite the good model fit at the county level, the DMSP-OLS images cannot perfectly predict economic activity due to their inherent limitations (e.g. low spatial resolution, lack of onboard and inter-satellite calibration, and limited dynamic range). In future studies, the assessment results need to be validated against additional datasets such as other NTL products (e.g. VIIRS images) or socio-economic data continuously collected during the disaster. Second, other factors that influence economic recovery should be taken into account in future studies. For instance, economic cycles (e.g. great recessions) can slow down business recovery after a disaster. In the introduced approach, linear models were used to generalize the economic growth in the pre- and post-Katrina periods, where the yearly fluctuations (e.g. the financial crisis in 2009) are averaged in the trend lines. Ideally, the “business-as-usual” trajectories should be projected with more sophisticated models to eliminate the effect of economic cycles. Third, the 20 selected variables can only explain ~40 % variation of the measured metrics, which reveal the complexity of community resilience. The prediction power of the model can be improved by including more variables and using more sophisticated model specifications (e.g. non-linear models). Robust models for community resilience prediction can be developed by accumulating empirical evidence in more disaster events.

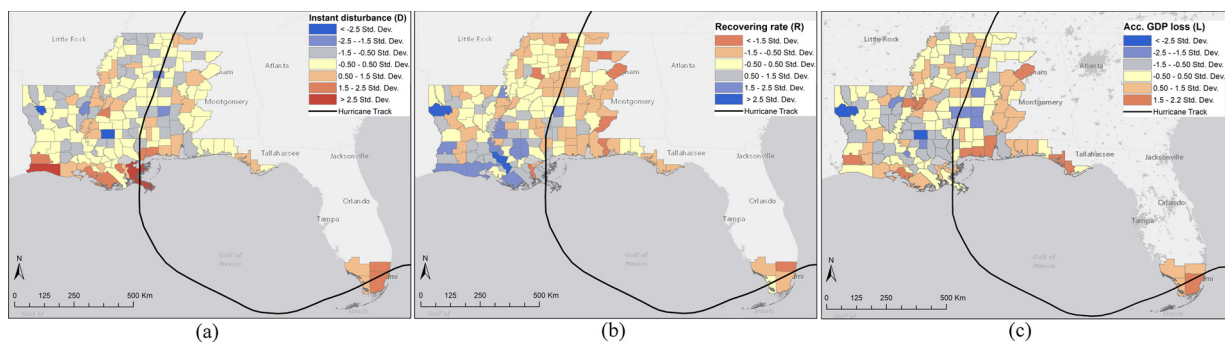


Fig. 7. Spatial variation of (a) instant disturbance (D), (b) recovering rate (R_r) and (c) accumulated GDP loss (L). Red indicates high instant disturbance (D), slower recovery (R_r) and high accumulated loss (L).

Table 3

Univariate regression analysis of instant disturbance (*D*), recovery (*R_r*) and economic loss (*L*) with environmental and socio-economic variables. Bold font indicates statistical significance ($p < 0.01$). Detailed statistics of the regression analysis (e.g. confidence intervals, standard errors of residuals, and residual distributions) can be found in the supplementary material.

Variable category	Variable	Instant disturbance (<i>D</i>)			Recovery rate (<i>R_r</i>)			Economic loss (<i>L</i>)		
		<i>b</i>	<i>p</i> value	<i>R</i> ²	<i>b</i>	<i>p</i> value	<i>R</i> ²	<i>b</i>	<i>p</i> value	<i>R</i> ²
Impact intensity	Max gust	0.272	0.000	0.074	0.000	0.995	0.000	0.046	0.545	0.002
	Rainfall	0.257	0.001	0.066	-0.064	0.393	0.004	0.053	0.477	0.003
Environment	Mean elevation	-0.375	0.000	0.140	-0.336	0.000	0.113	-0.113	0.132	0.013
	Distance to Coast	-0.358	0.000	0.128	-0.252	0.001	0.063	-0.081	0.279	0.007
	% of urban in flood zone	0.346	0.000	0.146	0.117	0.122	0.015	0.239	0.003	0.056
Socio-economic	% White	0.026	0.733	0.001	-0.057	0.447	0.003	0.013	0.867	0.000
	% Black	-0.060	0.425	0.004	0.068	0.369	0.005	-0.041	0.583	0.002
	% Asian	0.420	0.000	0.176	-0.083	0.271	0.007	0.333	0.000	0.111
	% Hispanic & Latino	0.299	0.000	0.089	-0.139	0.064	0.019	0.213	0.004	0.045
	% children	0.086	0.250	0.007	-0.257	0.001	0.066	0.255	0.001	0.065
	% elderly adult	0.083	0.267	0.007	-0.267	0.000	0.071	0.248	0.001	0.061
	% owner occupied homes	-0.274	0.000	0.075	0.126	0.092	0.016	-0.338	0.000	0.114
	% bachelor degree	0.161	0.031	0.026	-0.102	0.172	0.011	0.203	0.006	0.041
	% poverty	-0.136	0.068	0.019	0.110	0.141	0.012	-0.129	0.086	0.017
	Per cap. income	0.243	0.001	0.059	-0.140	0.061	0.020	0.243	0.001	0.059
Industrial structure	% small businesses	-0.184	0.014	0.034	-0.116	0.123	0.013	-0.085	0.259	0.007
	% large businesses	0.090	0.231	0.008	-0.110	0.143	0.012	0.142	0.057	0.020
	% Agriculture	-0.321	0.000	0.103	-0.116	0.121	0.014	-0.243	0.001	0.059
	% Mining	0.084	0.263	0.007	0.404	0.000	0.163	-0.214	0.004	0.046
	% Manufacture	-0.154	0.040	0.024	-0.077	0.303	0.006	-0.088	0.243	0.008

Table 4

Adjusted *R*² of the multivariate regressions between the resilience metrics (*D*, *R_r*, and *L*) and variables in different categories.

Variable category	Instant disturbance (<i>D</i>)		Recovery rate (<i>R_r</i>)		Economic loss (<i>L</i>)	
	<i>R</i> ²	Adj. <i>R</i> ²	<i>R</i> ²	Adj. <i>R</i> ²	<i>R</i> ²	Adj. <i>R</i> ²
All variables	0.399	0.327	0.369	0.293	0.274	0.187
Impact intensity	0.076	0.065	0.016	0.004	0.003	-0.008
Environmental	0.188	0.172	0.089	0.071	0.056	0.038
Socio-economic	0.286	0.243	0.099	0.045	0.246	0.201
Industrial structure	0.138	0.114	0.194	0.170	0.114	0.088

6. Conclusion

This study introduces a quantitative framework for resilience assessment using DMSP-OLS Nighttime Lights images. The framework was applied to model the recovery patterns of economic activity in the affected area in Hurricane Katrina 2005. The analyses show the great economic disturbance caused by Katrina and the slow recovery in the entire affected area. The county-level analyses indicate strong spatial variation of the recovery pattern. Statistical analyses were carried out to explore the underlying factors that influence the recovery patterns. This study demonstrates the utility of NTL images in monitoring human dynamics in natural disasters, which filled the critical gap of empirical data and assessment methods for resilience research. Based on the framework of recovery trajectory, resilience is modelled as a dynamic process. Compared with the traditional resilience indices, the modeling results can provide more specific and actionable measures to promote resilience in diverse communities and in different phases of a disaster. This study re-visits Hurricane Katrina using DMSP-OLS NTL images. However, the assessment approach is applicable for other disaster events using other NTL products (e.g. VIIRS DNB images). The results increase our understanding about the complexity of community resilience and provide support for decision-makers to develop resilient and sustainable communities.

Funding source

This article is based on work supported by two research grants from the U.S. National Science Foundation: one under the Coastlines and People (CoPe) Program (Award No. 1940091) and the other under the Methodology, Measurement & Statistics (MMS) Program (Award No. 1853866). Any opinions, findings, and conclusions or recommendations expressed in this material are those of the authors and do not necessarily reflect the views of the funding agencies.

Declaration of Competing Interests

The authors declare that they have no known competing financial interests or personal relationships that could have appeared to influence the work reported in this paper.

Appendix A. Supplementary data

Supplementary material related to this article can be found, in the online version, at doi:<https://doi.org/10.1016/j.scs.2020.102115>.

References

- Adeola, F. O. (2009). Mental health & psychosocial distress sequelae of Katrina: An empirical study of survivors. *Human Ecology Review*, 16, 195–210.
- Adger, W. N. (2000). Social and ecological resilience: Are they related? *Progress in Human Geography*, 24, 347–364. <https://doi.org/10.1191/030913200701540465>.
- Baade, R. A., Baumann, R., & Matheson, V. (2007). Estimating the economic impact of natural and social disasters, with an application to hurricane Katrina. *Urban Studies*, 44, 2061–2076. <https://doi.org/10.1080/00420980701518917>.
- Bakkensen, L. A., Fox-Lent, C., Read, L. K., & Linkov, I. (2017). Validating resilience and vulnerability indices in the context of natural disasters. *Risk Analysis*, 37, 982–1004. <https://doi.org/10.1111/risa.12677>.
- Bates, P. D. (2004). Remote sensing and flood inundation modelling. *Hydrological Processes*, 18, 2593–2597. <https://doi.org/10.1002/hyp.5649>.
- Beccari, B. (2016). A comparative analysis of disaster risk, vulnerability and resilience composite indicators. *PLOS Currents Disasters*. <https://doi.org/10.1371/currents.dis.453df025e34b682e973795070f9b970>.
- Bureau of Economic Analysis, U.S. Department of Commerce (2018). *Prototype gross domestic product by county*. 2012–2015.
- Bureau of Economic Analysis, U.S. Department of Commerce (2015). *Gross domestic product by state*. Advance 2014 and Revised 1997–2013.
- Burren, D., & Neusser, K. (2010). The decline in volatility of US GDP growth. *Applied Economics Letters*, 17, 1625–1631. <https://doi.org/10.1080/13504850903085050>.
- Burton, A. (2006). Health disparities: Crisis not over for hurricane victims. *Environmental Health Perspectives*, 114, A462.
- Cai, H., Lam, N. S. N., Zou, L., & Qiang, Y. (2018). Modeling the dynamics of community resilience to coastal hazards using a bayesian network. *Annals of the American Association of Geographers*, 108, 1260–1279. <https://doi.org/10.1080/24694452.2017.1421896>.
- Cooner, A. J., Shao, Y., & Campbell, J. B. (2016). Detection of urban damage using remote sensing and machine learning algorithms: Revisiting the 2010 Haiti earthquake. *Remote Sensing*, 8, 868. <https://doi.org/10.3390/rs8100868>.
- Cutter, S. L., Ash, K. D., & Emrich, C. T. (2014). The geographies of community disaster resilience. *Global Environmental Change: Human and Policy Dimensions*, 29, 65–77. <https://doi.org/10.1016/j.gloenvcha.2014.08.005>.
- Cutter, S. L., Barnes, L., Berry, M., Burton, C., Evans, E., Tate, E., et al. (2008). A place-based model for understanding community resilience to natural disasters. *Global Environmental Change: Human and Policy Dimensions*, 18, 598–606. <https://doi.org/10.1016/j.gloenvcha.2008.07.013>.
- Cutter, S. L., Boruff, B. J., & Shirley, W. L. (2003). Social vulnerability to environmental hazards. *Social Science Quarterly*, 84, 242–261. <https://doi.org/10.1111/1540-6237.8402002>.
- Cutter, S. L., Burton, C. G., & Emrich, C. T. (2010). Disaster resilience indicators for benchmarking baseline conditions. *Journal of Homeland Security and Emergency Management*, 7, 14. <https://doi.org/10.2202/1547-7355.1732>.
- Dasgupta, S., Laplante, B., Murray, S., & Wheeler, D. (2011). Exposure of developing countries to sea-level rise and storm surges. *Climatic Change*, 106, 567–579. <https://doi.org/10.1007/s10584-010-9959-6>.
- Dong, L., & Shan, J. (2013). A comprehensive review of earthquake-induced building damage detection with remote sensing techniques. *ISPRS Journal of Photogrammetry and Remote Sensing*, 84, 85–99. <https://doi.org/10.1016/j.isprsjprs.2013.06.011>.
- Elvidge, C. D., Ziskin, D., Baugh, K. E., Tuttle, B. T., Ghosh, T., Pack, D. W., et al. (2009). A fifteen year record of global natural gas flaring derived from satellite data. *Energies*, 2, 595–622. <https://doi.org/10.3390/en20300595>.
- Faturechi, R., & Miller-Hooks, E. (2015). Measuring the performance of transportation infrastructure systems in disasters: A comprehensive review. *Journal of Infrastructure Systems*, 21, 04014025. [https://doi.org/10.1061/\(ASCE\)IS.1943-555X.0000212](https://doi.org/10.1061/(ASCE)IS.1943-555X.0000212).
- Ferrara, L., Marcellino, M., & Mogliani, M. (2015). Macroeconomic forecasting during the Great Recession: The return of non-linearity? *International Journal of Forecasting*, 31, 664–679. <https://doi.org/10.1016/j.ijforecast.2014.11.005>.
- Finch, C., Emrich, C. T., & Cutter, S. L. (2010). Disaster disparities and differential recovery in New Orleans. *Population and Environment*, 31, 179–202. <https://doi.org/10.1007/s11111-009-0099-8>.
- Foster, K. (2012). In search of regional resilience. In M. Weir, H. Wial, & H. Wolman (Eds.). *Building regional resilience: Urban and regional policy and its effects*. Washington, DC: Brookings Institute Press.
- Fussell, E., Curtis, K. J., & DeWaard, J. (2014). Recovery migration to the City of New Orleans after Hurricane Katrina: A migration systems approach. *Population and Environment*, 35, 305–322. <https://doi.org/10.1007/s11111-014-0204-5>.
- Fussell, E., Sastry, N., & VanLandingham, M. (2010). Race, socioeconomic status, and return migration to New Orleans after Hurricane Katrina. *Population and Environment*, 31, 20–42. <https://doi.org/10.1007/s11111-009-0092-2>.
- Gillespie, T. W., Frankenberg, E., Chum, K. F., & Thomas, D. (2014). Nighttime lights time series of tsunami damage, recovery, and economic metrics in Sumatra. *Indonesia Remote Sensing Letter Print*, 5, 286–294. <https://doi.org/10.1080/2150704X.2014.900205>.
- Holling, C. S. (1973). Resilience and stability of ecological systems. *Annual Review of Ecology and Systematics*, 4, 1–23. <https://doi.org/10.1146/annurev.es.04.110173.000245>.
- Hong, Y., Adler, R., & Huffman, G. (2007). Use of satellite remote sensing data in the mapping of global landslide susceptibility. *Natural Hazards*, 43, 245–256. <https://doi.org/10.1007/s11069-006-9104-z>.
- Hsu, F.-C., Baugh, K. E., Ghosh, T., Zhizhin, M., & Elvidge, C. D. (2015). DMSP-OLS radiance calibrated nighttime lights time series with intercalibration. *Remote Sensing*, 7, 1855–1876. <https://doi.org/10.3390/rs70201855>.
- Huang, Q., Yang, X., Gao, B., Yang, Y., & Zhao, Y. (2014). Application of DMSP/OLS nighttime light images: A meta-analysis and a systematic literature review. *Remote Sensing*, 6, 6844–6866. <https://doi.org/10.3390/rs6086844>.
- Huang, X., Wang, C., & Lu, J. (2019). Understanding spatiotemporal development of human settlement in hurricane-prone areas on U.S. Atlantic and gulf coasts using nighttime remote sensing. *Natural Hazards and Earth System Sciences Discussions*. <https://doi.org/10.5194/nhess-2019-64>. Discuss. 1–22.
- Hultquist, C., Simpson, M., Cervone, G., & Huang, Q. (2015). Using nightlight remote sensing imagery and twitter data to study power outages, in: Proceedings of the 1st ACM SIGSPATIAL international workshop on the use of GIS in emergency management, EM-GIS' 15. ACM, New York, NY, USA. <https://doi.org/10.1145/2835596.2835601> pp. 6:1–6:6.
- Hung, H.-C., Yang, C.-Y., Chien, C.-Y., & Liu, Y.-C. (2016). Building resilience: Mainstreaming community participation into integrated assessment of resilience to climatic hazards in metropolitan land use management. *Land Use Policy*, 50, 48–58. <https://doi.org/10.1016/j.landusepol.2015.08.029>.
- Jonkman, S. N., Maaskant, B., Boyd, E., & Levitan, M. L. (2009). Loss of life caused by the flooding of New Orleans after hurricane Katrina: Analysis of the relationship between flood characteristics and mortality. *Risk Analysis*, 29, 676–698. <https://doi.org/10.1111/j.1539-6924.2008.01190.x>.
- Joshi, N., Baumann, M., Ehammer, A., Fensholt, R., Grogan, K., Hostert, P., et al. (2016). A review of the application of optical and radar remote sensing data fusion to land use mapping and monitoring. *Remote Sensing*, 8, 70. <https://doi.org/10.3390/rs8010070>.
- Knobb, R. D., Rhome, J. R., & Brown, R. D. (2005). *Tropical Cyclone Report: Hurricane Katrina* NOAA National Hurricane Center https://www.nhc.noaa.gov/data/tcr/AL122005_Katrina.pdf.
- Kohiyama, M., Hayashi, H., Maki, N., Higashida, M., Kroehl, H. W., Elvidge, C. D., et al. (2004). Early damaged area estimation system using DMSP-OLS night-time imagery. *International Journal of Remote Sensing*, 25, 2015–2036. <https://doi.org/10.1080/01431160310001595033>.
- Koliou, M., Lindt, J. W., van de, McAllister, T. P., Ellingwood, B. R., Dillard, M., & Cutler, H. (2018). State of the research in community resilience: Progress and challenges. *Sustain. Resilient Infrastruct.*, 0, 1–21. <https://doi.org/10.1080/23789689.2017.1418547>.
- Kuffer, M., Pfeffer, K., & Sliuzas, R. (2016). Slums from space—15 years of slum mapping using remote sensing. *Remote Sensing*, 8, 455. <https://doi.org/10.3390/rs8060455>.
- Lam, N. S. N., Pace, K., Campanella, R., LeSage, J., & Arenas, H. (2009). Business return in New Orleans: Decision making amid post-katrina uncertainty. *PLoS One*, 4, e6765. <https://doi.org/10.1371/journal.pone.0006765>.
- Lam, N. S.-N., Qiang, Y., Arenas, H., Brito, P., & Liu, K.-B. (2015). Mapping and assessing coastal resilience in the Caribbean region. *Cartography and Geographic Information Science*, 406, 1–8. <https://doi.org/10.1080/15230406.2015.1040999>.
- Lam, N. S. N., Reams, M., Li, K., Li, C., & Mata, L. P. (2016). Measuring community resilience to coastal hazards along the Northern Gulf of Mexico. *Natural Hazards Review*, 17. [https://doi.org/10.1061/\(ASCE\)NH.1527-6996.0000193](https://doi.org/10.1061/(ASCE)NH.1527-6996.0000193) e193.
- LeSage, J. P., Pace, R. K., Lam, N., Campanella, R., & Liu, X. (2011). New Orleans business recovery in the aftermath of Hurricane Katrina. *Journal of the Royal Statistical Society Series A*, 174, 1007–1027. <https://doi.org/10.1111/j.1467-985X.2011.00712.x>.
- Li, S., Dragicevic, S., Castro, F. A., Sester, M., Winter, S., Coltekin, A., et al. (2016). Geospatial big data handling theory and methods: A review and research challenges. *ISPRS Journal of Photogrammetry and Remote Sensing*, 115, 119–133. <https://doi.org/10.1016/j.isprsjprs.2015.10.012> Theme issue “State-of-the-art in photogrammetry, remote sensing and spatial information science”.
- Li, X., Ge, L., & Chen, X. (2013). Detecting Zimbabwe's decadal economic decline using nighttime light imagery. *Remote Sensing*, 5, 4551–4570. <https://doi.org/10.3390/rs5094551>.
- Li, X., Zhan, C., Tao, J., & Li, L. (2018). Long-term monitoring of the impacts of disaster on human activity using DMSP/OLS nighttime light data: A case study of the 2008 wenchuan, china earthquake. *Remote Sensing*, 10, 588. <https://doi.org/10.3390/rs10040588>.
- Liao, K.-H. (2012). A theory on urban resilience to floods—A basis for alternative planning practices. *Ecology and Society*, 17. <https://doi.org/10.5751/ES-05231-170448>.
- Marcellino, M. (2008). A linear benchmark for forecasting GDP growth and inflation? *Journal of Forecasting*, 27, 305–340. <https://doi.org/10.1002/for.1059>.
- Martin, R., & Sunley, P. (2015). On the notion of regional economic resilience: Conceptualization and explanation. *Journal of Economic Geography*, 15, 1–42. <https://doi.org/10.1093/jeg/ibu015>.
- Nicholls, R. J., Hoozemans, F. M. J., & Marchand, M. (1999). Increasing flood risk and wetland losses due to global sea-level rise: Regional and global analyses. *Global Environmental Change*, 9, S69–S87. [https://doi.org/10.1016/S0959-3780\(99\)00019-9](https://doi.org/10.1016/S0959-3780(99)00019-9).
- NOAA (2006). *Service assessment: Hurricane katrina August. 23-31, 2005*.
- Norris, F. H., Stevens, S. P., Pfefferbaum, B., Wyche, K. F., & Pfefferbaum, R. L. (2008). Community resilience as a metaphor, theory, set of capacities, and strategy for disaster readiness. *American Journal of Community Psychology*, 41, 127–150. <https://doi.org/10.1007/s10464-007-9156-6>.
- Peacock, W. G. (2010). *Final report advancing the resilience of coastal localities 10-02R*.
- Perz, S. G., Muñoz-Carpena, R., Kiker, G., & Holt, R. D. (2013). Evaluating ecological resilience with global sensitivity and uncertainty analysis. *Ecological Modelling*, 263, 174–186. <https://doi.org/10.1016/j.ecolmodel.2013.04.024>.
- Peterson, J. S., Stanley, L. D., Glazier, E., & Philipp, J. (2006). A preliminary assessment of social and economic impacts associated with hurricane Katrina. *American Anthropologist*, 108, 643–670. <https://doi.org/10.1525/aa.2006.108.4.643>.
- Qiang, Y. (2019). Disparities of population exposed to flood hazards in the United States. *Journal of Environmental Management*, 232, 295–304. <https://doi.org/10.1016/j.jem>.

- jenvman.2018.11.039.
- Qiang, Y., & Lam, N. S.-N. (2016). The impact of Hurricane Katrina on urban growth in Louisiana: An analysis using data mining and simulation approaches. *International Journal of Geographical Information Science*, *30*, 1832–1852. <https://doi.org/10.1080/13658816.2016.1144886>.
- Qiang, Y., & Xu, J. (2019). Empirical assessment of road network resilience in natural hazards using crowdsourced traffic data. *International Journal of Geographical Information Science*, 1–17. <https://doi.org/10.1080/13658816.2019.1694681>.
- Sastry, N., & VanLandingham, M. (2009). One year later: Mental illness prevalence and disparities among new orleans residents displaced by hurricane katrina. *American Journal of Public Health*, *99*, S725–S731. <https://doi.org/10.2105/AJPH.2009.174854>.
- Sempier, T. T., Swann, D. L., Emmer, R., Sempier, S. H., & Schneider, M. (2010). *Coastal community resilience index: A community self-assessment (No. MASGP-08-014)*.
- Shahtahmassebi, A. R., Song, J., Zheng, Q., Blackburn, G. A., Wang, K., Huang, L. Y., et al. (2016). Remote sensing of impervious surface growth: A framework for quantifying urban expansion and re-densification mechanisms. *International Journal of Applied Earth Observation and Geoinformation*, *46*, 94–112. <https://doi.org/10.1016/j.jag.2015.11.007>.
- Sherrieb, K., Norris, F. H., & Galea, S. (2010). Measuring capacities for community resilience. *Social Indicators Research*, *99*, 227–247. <https://doi.org/10.1007/s11205-010-9576-9>.
- Spalding, M. D., McIvor, A. L., Beck, M. W., Koch, E. W., Möller, I., Reed, D. J., et al. (2014). Coastal ecosystems: A critical element of risk reduction. *Conservation Letters*, *7*, 293–301. <https://doi.org/10.1111/conl.12074>.
- Tebaldi, C., Strauss, B. H., & Zervas, C. E. (2012). Modelling sea level rise impacts on storm surges along US coasts. *Environmental Research Letters*, *7*, 014032. <https://doi.org/10.1088/1748-9326/7/1/014032>.
- Timmerman, P. (1981). *Vulnerability, resilience and the collapse of society - a review of models and possible climatic applications*. University of Toronto Institute For Environmental Studies Environmental Monograph. Institute for Environmental Studies, University of Toronto.
- U.S. Census (2019). *American community survey*.
- U.S. Census Bureau (2011). *Census 2010*. U.S. Census Bureau.
- Vercelloni, J., Kayal, M., Chancerelle, Y., & Planes, S. (2019). Exposure, vulnerability, and resiliency of French Polynesian coral reefs to environmental disturbances. *Scientific Reports*, *9*, 1027. <https://doi.org/10.1038/s41598-018-38228-5>.
- Vetrivel, A., Gerke, M., Kerle, N., Nex, F., & Vosselman, G. (2018). Disaster damage detection through synergistic use of deep learning and 3D point cloud features derived from very high resolution oblique aerial images, and multiple-kernel-learning. *ISPRS Journal of Photogrammetry and Remote Sensing*, *140*, 45–59. <https://doi.org/10.1016/j.isprsjprs.2017.03.001> Geospatial Computer Vision.
- Vu, L., VanLandingham, M. J., Do, M., & Bankston, C. L. (2009). Evacuation and return of vietnamese new orleanians affected by hurricane katrina. *Organization & Environment*, *22*, 422–436. <https://doi.org/10.1177/1086026609347187>.
- White, R. K., Edwards, W. C., Farrar, A., & Plodinec, M. J. (2015). A practical approach to building resilience in America's communities. *The American Behavioral Scientist*, *59*, 200–219. <https://doi.org/10.1177/0002764214550296>.
- World Bank (2019). *World Bank national accounts data*.
- Xie, Y., & Weng, Q. (2017). Spatiotemporally enhancing time-series DMSP/OLS nighttime light imagery for assessing large-scale urban dynamics. *ISPRS Journal of Photogrammetry and Remote Sensing*, *128*, 1–15. <https://doi.org/10.1016/j.isprsjprs.2017.03.003>.
- Yodo, N., & Wang, P. (2016). Engineering resilience quantification and system design implications: A literature survey. *Journal of Mechanical Design*, *138*. <https://doi.org/10.1115/1.4034223>.
- Zhao, X., Yu, B., Liu, Y., Yao, S., Lian, T., Chen, L., et al. (2018). NPP-VIIRS DNB daily data in natural disaster assessment: Evidence from selected case studies. *Remote Sensing*, *10*, 1526. <https://doi.org/10.3390/rs10101526>.
- Zhuo, L., Ichinose, T., Zheng, J., Chen, J., Shi, P. J., & Li, X. (2009). Modelling the population density of China at the pixel level based on DMSP/OLS non-radiance-calibrated night-time light images. *International Journal of Remote Sensing*, *30*, 1003–1018. <https://doi.org/10.1080/01431160802430693>.
- Zou, L., Lam, N. S.-N., Cai, H., & Qiang, Y. (2018). Mining twitter data for improved understanding of disaster resilience. *Annals of the American Association of Geographers*, *108*(5), 1422–1441. <https://doi.org/10.1080/24694452.2017.1421897>.
- Zou, L., Lam, N. S. N., Shams, S., Cai, H., Meyer, M. A., Yang, S., et al. (2018). Social and geographical disparities in Twitter use during Hurricane Harvey. *International Journal of Digital Earth*, 1–19. <https://doi.org/10.1080/17538947.2018.1545878>.